

1

2 **Evidence that ice forms primarily in supercooled liquid clouds at temperatures  $> -27^{\circ}\text{C}$**

3 C. D. Westbrook and A. J. Illingworth

4 **Abstract:**

5 Using 4 years of radar and lidar observations of layer clouds from the Chilbolton Observatory  
6 in the UK, we show that almost all (95%) ice particles formed at temperatures  $> -20^{\circ}\text{C}$  appear  
7 to originate from supercooled liquid clouds. At colder temperatures, there is a monotonic  
8 decline in the fraction of liquid-topped ice clouds: 50% at  $-27^{\circ}\text{C}$ , falling to zero at  $-37^{\circ}\text{C}$   
9 (where homogeneous freezing of water droplets occurs). This strongly suggests that  
10 deposition nucleation plays a relatively minor role in the initiation of ice in mid-level clouds.  
11 It also means that the initial growth of the ice particles occurs predominantly within a liquid  
12 cloud, a situation which promotes rapid production of precipitation via the Bergeron-  
13 Findeison mechanism.

14

15

## 16 **1. Introduction**

17 The formation of ice in the troposphere is fundamental to the production of precipitation and  
18 the maintenance of the global water cycle. Yet this process remains one of the most poorly  
19 understood topics in cloud physics, and a major uncertainty in climate models (DeMott et al  
20 2010). Two key factors contributing to this uncertainty are: (i) we do not have a robust  
21 characterisation of the way ice is initially nucleated within clouds, and (ii) we do not know  
22 the environmental conditions in which the newly-formed ice particles grow, and therefore the  
23 rate at which precipitation-sized particles are produced. Clearly problems (i) and (ii) are  
24 intimately linked.

25 The relatively frequent occurrence of a thin layer of supercooled liquid water droplets at the  
26 top of ice-phase clouds has been observed in several cases (Rauber and Tokay 1991), but the  
27 fraction of ice clouds which have liquid water at the top has not yet been quantified.  
28 Recently, Ansmann et al (2009) analysed 4 weeks of observations of short-lived tropical  
29 altocumulus clouds and found that liquid droplets were always observed first, before the  
30 appearance of ice falling beneath: hence they inferred that deposition nucleation was  
31 unimportant in such clouds. Similarly, de Boer et al (2011) analysed low- and mid-level  
32 arctic clouds (<4km altitude) using coincident radar, lidar and radiosonde profiles. They  
33 show 6 case studies of vertically-pointing radar and lidar observations where liquid was  
34 observed overhead before the appearance of ice virga below, although one could argue that  
35 this might be due to wind shear near cloud top. They also highlighted one case where the air  
36 was supersaturated with respect to ice but below liquid water saturation: ice particles were  
37 absent, suggesting liquid droplets were needed for ice to form. Finally, they applied the  
38 classification scheme of Shupe (2007) to remote sensing observations over a longer period,

39 from 3 arctic sites, to conclude that liquid-topped ice clouds are the most common cloud type  
40 at temperatures between  $\approx -25$  and  $-10^{\circ}\text{C}$ .

41 The aim of this letter is to use long term radar and lidar observations from the Chilbolton  
42 Observatory in the UK to explicitly estimate the fraction of ice clouds (at all heights) which  
43 have liquid water at the top, and what this implies for ice nucleation and growth of  
44 precipitation-sized particles.

## 45 **2. Method**

46 Observations were made using the 8.6 and 3.2mm cloud radars (30s integration time, 60m  
47 gate length oversampled to 30m), and 905nm lidar (30s x 30m) at the Chilbolton Observatory  
48 in the UK. See Illingworth et al (2010) for more details of the instrument specifications. The  
49 lidar points  $4^{\circ}$  off zenith to avoid specular reflection from ice crystals. All data is interpolated  
50 on to a universal 30s x 30m grid and smoothed over 1.5 minutes.

51 The combination of millimetre radar and infrared lidar is a powerful one: it is well  
52 established (e.g. Hogan et al 2004) that lidar measurements are extremely sensitive to the  
53 presence of supercooled liquid water droplets, because although only  $\sim 10\mu\text{m}$  in diameter,  
54 they are present in large numbers ( $\sim 100\text{cm}^{-3}$ ). In contrast, at radar wavelengths backscatter  
55 from clouds containing only droplets is extremely weak ( $< -20\text{dBZ}$ : Khain et al 2008). The  
56 strong size dependence of Rayleigh scattering means that although the concentration of ice  
57 particles is typically 3-5 orders of magnitude lower than that of droplets, ice crystals are  
58 much more reflective, and dominate the radar signal when present (Westbrook et al 2010).  
59 An example 5 hour period from 25 June 2009 is shown in figure 1a,b, where ice particles are  
60 clearly observed falling from a thin supercooled layer cloud at 5000m altitude ( $-13^{\circ}\text{C}$ )  
61 between 1920 and 2040UTC. The lidar imagery shows a thin, highly reflective stripe at the  
62 top (the supercooled droplets, backscatter  $> 10^{-4}\text{m}^{-1}\text{sr}^{-1}$ ), whilst the radar shows the ice

63 particles within the supercooled layer, and falling below with characteristic fallstreak  
64 structure. Also shown in this time series are ice-only cirrus clouds (a tenuous layer at 2130-  
65 2200 UTC, top  $-37^{\circ}\text{C}$ ; and a deeper layer near midnight, top  $-45^{\circ}\text{C}$ ) – radar reflectivities  $Z$   
66 are within a similar range, but lidar backscatters are much lower, and there are no sharp  
67 gradients in the lidar signal.

68 Rather than analysing the radar and lidar observations profile-by-profile (ie. treating each  
69 profile as an independent cloud), discrete ‘layers’ of cloud are identified from the time series.  
70 This is done by looking for contiguous regions of radar reflectivity, and labelling each as a  
71 separate cloud. To determine if the layer contains ice, we look for clouds where  $Z > -20\text{dBZ}$   
72 for at least 15 rays (7.5 minutes). This  $Z$  threshold was chosen based on figure 1 of Khain et  
73 al (2008) which shows that cloud layers containing only droplets always have reflectivities  
74 less than this value.

75 To avoid misdiagnosis of drizzle drops as ice, only clouds with tops  $< -10^{\circ}\text{C}$  are included.  
76 Sensitivity tests (see section 4) confirm that our statistics are not affected by drizzle.

77 Following this segregation, each ice-containing cloud layer is searched for profiles where  
78 there is a lidar return ( $> 10^{-6}\text{m}^{-1}\text{sr}^{-1}$ ) within 90m of the radar echo top. This condition is an  
79 important one – if the lidar cannot penetrate to the top of the cloud layer, we cannot be sure  
80 whether liquid droplets are present or not, and we therefore throw away cloud layers for  
81 which this is not satisfied. This methodology distinguishes our statistical analysis from the  
82 classification of de Boer et al (2011), who applied Shupe’s (2007) classification scheme.  
83 Their scheme infers the presence of mixed-phase layers even when the lidar is extinguished,  
84 provided an elevated value ( $> 0.4\text{m/s}$ ) of radar Doppler spectral width is present. Spectral  
85 width is primarily an indicator of turbulence, and while it is certainly our experience that the  
86 top few hundred metres of mixed-phase clouds often have elevated levels of spectral width,

87 this is not always the case: for example no part of the mixed-phase cloud in figure 1 had  
88 spectral width values exceeding 0.4m/s. In addition, there are other situations (eg cirrus  
89 generating cells) where this turbulent threshold is exceeded. A more robust approach to  
90 quantifying the fraction of liquid-topped ice clouds therefore is to only consider cloud layers  
91 where the supercooled liquid (or lack of it) can be directly observed by lidar, and this is the  
92 approach we have taken in this work.

93 To determine whether a supercooled layer is present at the top of an ice cloud layer, we look  
94 for the sharp increase in backscatter produced at the base of a liquid cloud. Each lidar  
95 backscatter profile is searched for a gradient exceeding  $5 \times 10^{-7} \text{ m}^{-2} \text{ sr}^{-1}$  in the top 500m of the  
96 cloud layer, and the lowest range gate in which this occurs is identified as liquid cloud base.  
97 If liquid is observed at the top of the ice layer for at least 7.5 minutes, we diagnose it as  
98 ‘liquid-topped’. If liquid is not observed, but a detectable lidar signal (backscatter  $> 10^{-6} \text{ m}^{-1} \text{ sr}^{-1}$ )  
99 is obtained from cloud top for at least 7.5 minutes we diagnose it as ‘ice-topped’. These  
100 thresholds of 7.5 minutes mean that the minimum width of cloud layer included in the  
101 analysis is dependent on wind speed, but since most of our cloud layers persist for much  
102 longer than 7.5 minutes (see section 3) this is not expected to affect our statistics.

103 For the purpose of accumulating statistics as a function of cloud-top temperature, clouds  
104 where the top is highly variable in temperature (standard deviation for the complete cloud  
105 layer  $> 5^\circ\text{C}$ ) are discarded. The  $5^\circ\text{C}$  value was a compromise between restricting the analysis  
106 to well-defined layer clouds with flat-tops, whilst not rejecting upper-level cirrus clouds  
107 which are often less homogeneous. The temperature field for each day was obtained from the  
108 Met Office operational forecast model with 6-11 hour lead time. Errors in model temperature  
109 at a given level are expected to be small ( $\approx 1^\circ\text{C}$ : Mittermaier and Illingworth 2002) because of  
110 the regular assimilation of radiosonde profiles.

111 Figure 1c shows how the classification works in practice. The analysis was repeated for 1496  
112 days (4 years) of coincident radar and lidar observations made between 2003-2010 where  
113 radar and lidar were available. A total of 917 hours (110,000 30-s profiles) of ice-containing  
114 cloud layers which the lidar could penetrate to the cloud top were identified and analysed.  
115 The median depth of the liquid layers was 210m (derived from lidar-detected base and radar  
116 detected top).

### 117 **3. Results**

118 Figure 2 (square markers) shows the fraction of ice cloud layers which have supercooled  
119 liquid water at the top, as a function of cloud top temperature  $T$ . Each temperature bin  
120 contains approximately 40 separate cloud layers, persisting for an average of 1.5 hours each.  
121 Strikingly, when  $T > -20^{\circ}\text{C}$  we observe that almost every single ice cloud has supercooled  
122 liquid at the top. This is strong evidence that ice is produced via freezing of droplets in this  
123 temperature range, and that either deposition nucleation plays little role in the formation of  
124 ice at these temperatures, or that for some reason such nuclei can only become active in  
125 liquid clouds.

126 In colder clouds the fraction of liquid-topped cases falls off steadily. At  $-27^{\circ}\text{C}$  half of the ice  
127 cloud layers are liquid-topped; at  $-37^{\circ}\text{C}$  no liquid-topped clouds are detected. This is  
128 consistent with the onset of homogeneous freezing of cloud droplets at this temperature  
129 (Mason 1971). Note that the fractions in figure 2 are necessarily underestimates of the  
130 fraction of clouds which have had liquid water at the top at some point in their lifetime,  
131 because some clouds will have glaciated by the time they are observed, particularly at colder  
132 temperatures. This suggests then that ice nucleation *via* the liquid phase is extremely  
133 important for a wide range of temperatures: even in clouds as cold as  $-33^{\circ}\text{C}$ , liquid droplets  
134 are detected at the top in  $\approx 15\%$  of cases.

135 In addition to the implications for ice nucleation, there is also an important ramification for  
136 the initial growth and evolution of the ice crystals produced. Ice crystals growing in  
137 supercooled clouds do so at the maximum possible rate by vapour deposition, hence  
138 producing precipitation-sized particles more rapidly than would occur if nucleation were to  
139 occur at lower supersaturations. This should therefore focus our attention on characterising  
140 the vapour deposition growth rates in these highly supersaturated conditions.

#### 141 **4. Sensitivity tests**

142 We now test the use of the threshold  $Z > -20\text{dBZ}$  to diagnose the presence of ice. The first  
143 sensitivity test is to simply increase the threshold to  $-10\text{dBZ}$  to be completely sure that no  
144 liquid droplet clouds are being diagnosed as containing ice. The statistics obtained in this  
145 case are shown by the diamonds in figure 2. The data is slightly noisier because of the smaller  
146 sample (average of 15 layers per temperature bin, as few as 8 in high, cold clouds), but the  
147 result is essentially the same, suggesting that our diagnosis is robust.

148 A second test was carried out to determine whether supercooled drizzle might be mistaken for  
149 ice. Large drizzle drops, like ice crystals, have a significant radar cross section. To be sure  
150 that drizzle is not affecting our statistics in the warmer clouds, we have analysed a subset  
151 (861 days between 2006-2010) of the data where a second lidar pointing directly at zenith  
152 was also operating at Chilbolton. Using this data we can easily identify regions of cloud  
153 affected by specular reflection from oriented plate-like ice crystals (Westbrook et al 2010).  
154 Since we can be sure that clouds with this signature must contain ice, statistics were  
155 recomputed for layers where  $Z > -20\text{dBZ}$  and a layer of specular reflection at least 100m deep  
156 was also present. We focus on the temperature range between  $-10$  and  $-20^\circ\text{C}$  which are the  
157 warmest clouds in our analysis, and hence where drizzle would be most likely to form.  
158 Conveniently, this also the temperature range where the growth of plate-like crystals occurs

159 (Mason 1971). The results obtained when this more stringent condition is applied are shown  
160 by the triangles in figure 2: again the data are noisier because of the more limited sample, but  
161 we observe no significant change from the previous results.

162 We therefore conclude that our analysis is not sensitive to the thresholds used to diagnose the  
163 presence of ice.

## 164 **5. Conclusions and discussion**

165 The fraction of ice clouds which have a layer of supercooled liquid water at the top has been  
166 estimated from an extensive data set of collocated radar and lidar observations. The results  
167 strongly suggest that:

- 168 1. Supercooled liquid water occurs at the top of the majority of ice cloud layers warmer  
169 than  $-27^{\circ}\text{C}$ , and is almost always present when the cloud top temperature is greater  
170 than  $-20^{\circ}\text{C}$ .
- 171 2. From the lack of ice-only clouds we infer that deposition nucleation is weak in mid-  
172 level clouds, and that ice nucleation proceeds *via* the liquid phase at temperatures  $> -$   
173  $20^{\circ}\text{C}$ . This extends the inference made by Ansmann et al (2009) from 4 weeks of lidar  
174 observations, to a conclusion based on four years of continuous radar and lidar data.
- 175 3. The initial growth of ice crystals takes place in the presence of liquid droplets at  
176 temperatures  $> -27^{\circ}\text{C}$ , maximising the rate at which the ice particles grow and form  
177 precipitation.

178 Finally, we discuss the limitations of our analysis. First, it was necessary to remove clouds  
179 where the top temperature varied significantly. This is a frequent occurrence: many clouds  
180 associated with frontal systems are sloped, and multilayered clouds are also common - our  
181 analysis rejects these clouds. Second, the radar reflectivity threshold may well filter out cold

182 cirrus layers, simply because the particles are too small to pass the -20dBZ threshold (eg the  
183 layer at 2130-2200 UTC in figure 1). In future work we hope to investigate the sensitivity of  
184 our results to this using polarisation lidar, which is more sensitive to the presence of small  
185 crystals.

186 The influence of aerosols on the formation of ice has not been considered in this paper:  
187 segregating the data according to the origin of the air masses following Seifert et al (2010)  
188 may provide a means of assessing this.

189 The requirement that the lidar has to detect the top of the cloud layer inevitably means that  
190 the majority of clouds in our analysis have an optical depth through the ice-phase part of the  
191 cloud less than  $\sim 3$ ; likewise we cannot sample cold clouds which lie above low-level liquid  
192 clouds, or during rain. While we see no obvious argument that the nucleation characteristics  
193 of clouds obscured in this way would be different to the layers which we can see, it would be  
194 desirable to test this. Future work will focus on using space-borne radar and lidar to perform  
195 the same analysis, since any liquid at the top of the uppermost cloud layer is then easily  
196 detectable.

## 197 **Acknowledgements**

198 We are grateful to the staff at the STFC Chilbolton Observatory for operating the lidars and  
199 radars. This work was carried out as part of the Natural Environment Research Council  
200 APPRAISE-CLOUDS project, grant NE/EO11241.

## 201 **References**

202 Ansmann A, M Tesche, P Seifert, D Althausen, R Engelmann, J Fruntke, U Wandinger, I  
203 Mattis and D Müller (2009) Evolution of the ice phase in tropical altocumulus: SAMUM  
204 lidar observations over Cape Verde *J. Geophys. Res.* **114** D17208

205 de Boer G, H Morrison, MD Shupe and R Hildner (2011) Evidence of liquid-dependent ice  
206 nucleation in high-latitude stratiform clouds from surface remote sensors *Geophys. Res. Lett.*  
207 **38** L01803

208 DeMott PJ et al (2010) Predicting global atmospheric ice nuclei distributions and their  
209 impacts on climate *Proc. Nat. Acad. Sci. (USA)* **107** 11217-11222

210 Hogan RJ, MD Behera, EJ O'Connor and AJ Illingworth 2004 Estimating the global  
211 distribution of supercooled liquid water clouds using spaceborne lidar *Geophys. Res. Lett.* **32**  
212 L05106

213 Illingworth AJ, RJ Hogan, EJ O'Connor, D Bouniol et al 2007 Cloudnet – continuous  
214 evaluation of cloud profiles in seven operational models using ground-based observations  
215 *Bull. Amer. Meteorol. Soc.* **88** 883-898

216 Khain A et al (2008) Combined observational and model investigations of the Z-LWC  
217 relationship in stratocumulus clouds *J. Appl. Met. & Clim.* **47** 591-606

218 Mason (1971) *The physics of clouds* second edition, Oxford University Press.

219 Mittermaier MP and AJ Illingworth (2003) Comparison of model-derived and radar-observed  
220 freezing level heights: implications for vertical reflectivity profile correction schemes

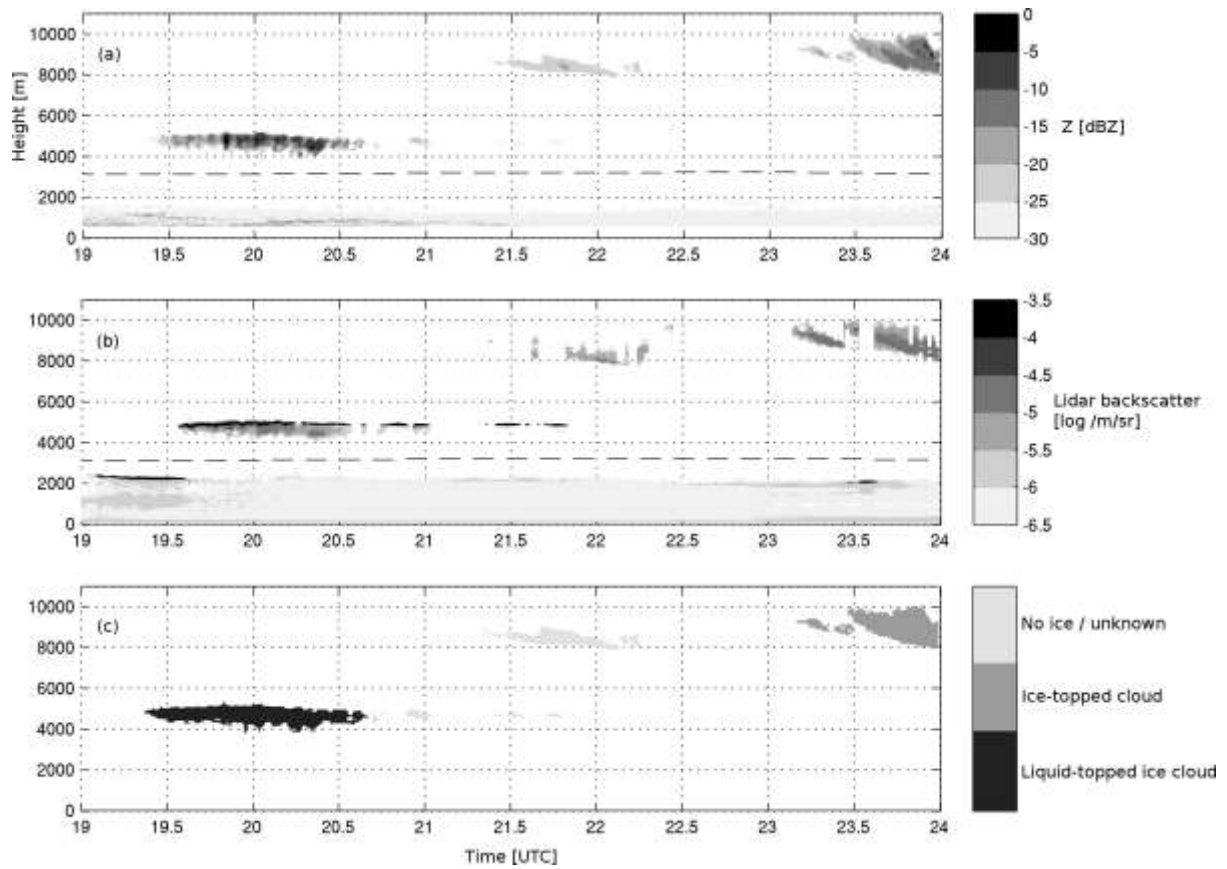
221 Rauber RM and A Tokay 1991 An explanation for the existence of supercooled water at the  
222 top of cold clouds *J. Atmos. Sci.* **48** 1005-1023

223 Seifert P et al 2010 Saharan dust and heterogeneous ice formation: eleven years of cloud  
224 observations at a central European EARLINET site *J. Geophys. Res.* **115** D20201

225 Shupe MD (2007) A ground-based multisensor cloud phase classifier *Geophys. Res. Lett.* **34**  
226 L22809

227 Westbrook CD, AJ Illingworth, RJ Hogan and EJ O'Connor (2010) Doppler lidar  
228 measurements of oriented planar ice crystals falling from supercooled and glaciated cloud  
229 layers *Q. J. R. Meteorol. Soc.* **136** 260-276

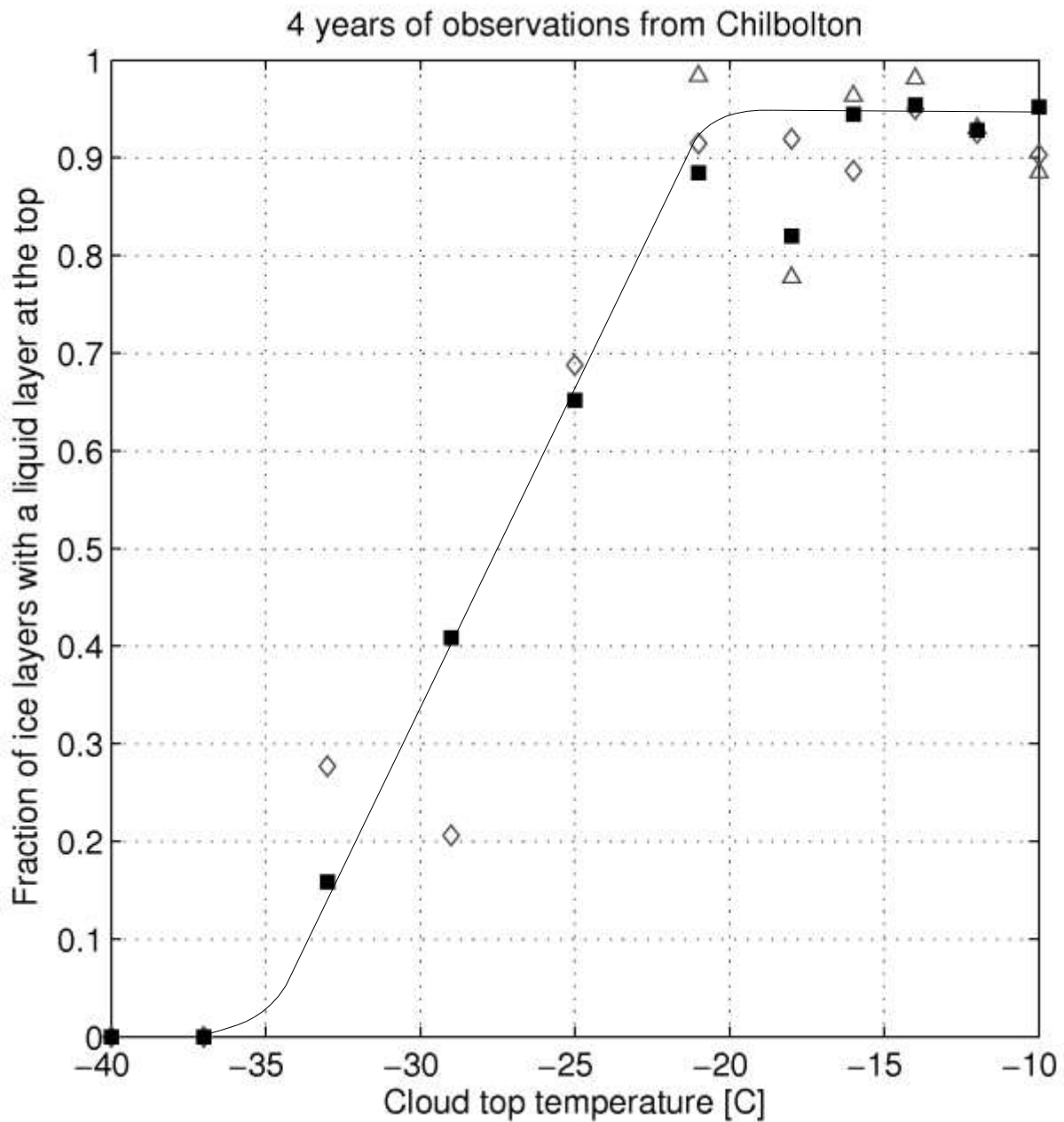
230



232

233 Figure 1: example of cloud observations from 25 June 2009: (a) radar reflectivity, (b) lidar  
 234 backscatter, (c) classification of cloud layers into liquid-topped ice clouds, ice-topped clouds,  
 235 and clouds which do not contain ice, whose phase is uncertain, or whose top varies by  
 236 undulates by more than  $5^{\circ}\text{C}$ . Dashed line in panels (a,b) indicates  $0^{\circ}\text{C}$  isotherm: below this  
 237 level weak radar returns from insects and lidar returns from boundary layer aerosol/cloud are  
 238 visible - these features are not included in our analysis.

239



241

242 Figure 2: Fraction of ice-phase cloud layers which also have supercooled liquid water  
 243 droplets at the top, as a function of cloud top temperature (filled black squares). The solid line  
 244 is intended to guide the eye. Gray symbols are results of sensitivity tests where: threshold for  
 245 diagnosis of ice particles is increased to -10dBZ (diamonds); specular reflection from  
 246 oriented ice crystals is needed for diagnosis of ice (triangles). See text for more details.